Nitric Oxide 153 (2024) 50–60

Contents lists available at ScienceDirect

Nitric Oxide

journal homepage: www.elsevier.com/locate/yniox

Trial of the cerebral perfusion response to sodium nitrite infusion in patients with acute subarachnoid haemorrhage using arterial spin labelling MRI

Martyn Ezra [a,*], Edit Franko [a], Desiree B. Spronk [a], Catherine Lamb [b], Thomas W. Okell [c], Kyle TS. Pattinson [a]

[a] Nuffield Division of Anaesthetics, Nuffield Department of Clinical Neurosciences, University of Oxford, Oxford, UK
[b] Neuro Intensive Care Unit, John Radcliffe Hospital, Oxford University Hospitals NHS Foundation Trust, Oxford, UK
[c] Wellcome Centre for Integrative Neuroimaging, FMRIB, Nuffield Department of Clinical Neurosciences, University of Oxford, Oxford, UK

ARTICLE INFO

Keywords:
Nitrite
Subarachnoid haemorrhage stroke
Nitric oxide
Cerebral blood flow
Arterial spin labelling

ABSTRACT

Aneurysmal subarachnoid haemorrhage (SAH) is a devastating subset of stroke. One of the major determinants of outcome is an evolving multifactorial injury occurring in the first 72 hours, known as early brain injury. Reduced nitric oxide (NO) bioavailability and an associated disruption to cerebral perfusion is believed to play an important role in this process. We sought to explore this relationship, by examining the effect on cerebral perfusion of the *in vivo* manipulation of NO levels using an exogenous NO donor (sodium nitrite).

We performed a double blind placebo controlled randomised experimental medicine study of the cerebral perfusion response to sodium nitrite infusion during the early brain injury period in 15 low grade (World Federation of Neurosurgeons grade 1–2) SAH patients. Patients were randomly assigned to receive sodium nitrite at 10 mcg/kg/min or saline placebo. Assessment occurred following endovascular aneurysm occlusion, mean time after ictus 66h (range 34–90h). Cerebral perfusion was quantified before infusion commencement and after 3 hours, using multi-post labelling delay (multi-PLD) vessel encoded pseudocontinuous arterial spin labelling (VEPCASL) magnetic resonance imaging (MRI).

Administration of sodium nitrite was associated with a significant increase in average grey matter cerebral perfusion. Group level voxelwise analysis identified that increased perfusion occurred within regions of the brain known to exhibit enhanced vulnerability to injury. These findings highlight the role of impaired NO bioavailability in the pathophysiology of early brain injury.

1. Introduction

Aneurysmal subarachnoid haemorrhage (SAH) is a devastating subset of stroke, associated with significant morbidity and mortality [1]. SAH is estimated to cost the UK £510 million per year, with the loss of productive years approaching that of ischaemic stroke [2]. One of the major determinants of patient outcome is the development of delayed secondary neurological injuries, 3–14 days after the initial bleed, known as delayed cerebral ischemia (DCI) [3]. Impaired cerebral blood flow during the first 72 hours following aneurysmal rupture, a period known as early brain injury (EBI), is thought to play a critical role in the development of DCI [4–19].

Following SAH there is a profound disruption to the cerebral nitric oxide (NO) signalling pathways [20]. NO is a potent vasodilator, involved in the maintenance of basal vascular tone and the regulation of cerebral blood flow. Reduced NO bioavailability following SAH may, therefore, play a critical role in pathophysiology of EBI. However, clinical studies attempting to correlating changes in cerebrospinal fluid NO metabolites during EBI with the development of DCI have failed to demonstrate a clear association [21–24]. Whilst this likely reflects the difficulty in extrapolating NO metabolite levels to the biological availability of NO, the role of NO in the pathophysiology of EBI remains uncertain.

In a series of studies our group has sought to determine the role of NO in the pathophysiology of EBI utilising a novel experimental medicine approach. Using sodium nitrite as an endogenous NO donor, the effects

* Corresponding author. Nuffield Department of Clinical Neurosciences, John Radcliffe Hospital, Oxford, OX3 9DU, UK.
E-mail address: martyn.ezra@ndcn.ox.ac.uk (M. Ezra).

https://doi.org/10.1016/j.niox.2024.10.003
Received 24 April 2024; Received in revised form 3 October 2024; Accepted 3 October 2024
Available online 5 October 2024

of *in vivo* NO level manipulation were examined in SAH patients during EBI. Sodium nitrite administration was shown to increase the electroencephalographic (EEG) spectral alpha/delta power ratio (ADR) (a marker of cerebral ischemia) and normalise the low frequency synchronisation between arterial blood pressure and transcranial doppler (TCD) derived cerebral blood flow velocity (a marker of cerebral vascular function) [25–27]. Exogenous NO administration, therefore, appears to normalise cerebrovascular function and improve cerebral perfusion during EBI.

Whilst these findings support the role of reduced NO bioavailability in the pathophysiology of EBI, they represent indirect measures of cerebral blood flow and are therefore subject to a range of confounding factors. As such, quantitative assessment of the cerebral blood flow response to sodium nitrite is required.

Arterial spin labelling (ASL) magnetic resonance imaging (MRI) is a completely non-invasive method for imaging perfusion in the brain that uses blood water as an endogenous tracer. It is therefore ideally suited for experimental designs where repeated perfusion measurement is required. Recent developments in ASL sequences have enabled estimation of cerebral perfusion from the different feeding arteries of the brain. Vessel encoded labelling techniques improves absolute quantification of perfusion in the presence of altered blood arrival times, especially in regions supplied by two different vascular territories with different vessel arrival times [28]. This has been identified as a significant factor limiting the utility of conventional ASL in patients with SAH [29].

The aim of this study was to determine the effect of the administration of sodium nitrite on cerebral perfusion during EBI following SAH, using a double-blind placebo controlled randomised study design and state-of-the-art vessel encoded ASL imaging. We hypothesised that sodium nitrite administration would be associated with an increase in cerebral perfusion, further demonstrating the role of functional NO depletion in the pathophysiology of EBI.

2. Methods

2.1. Participants

All patients aged 18–80 years admitted to the John Radcliffe Hospital, Oxford between April 2016 and June 2018, having suffered low grade aneurysmal SAH (WFNS (World Federation of Neurosurgeons) grade 1–2) and successfully treated with endovascular coiling, were assessed for eligibility for inclusion in this study. Inclusion was dependent on the ability to perform the first MRI within 96 hours of ictus and the second MRI 3 hours after commencement of the drug infusion protocol. Ictus was defined as primary headache associated with medical intervention.

Exclusion criteria included contraindications to sodium nitrite, pre-existing methaemoglobinaemia, history of glucose-6-phosphate dehydrogenase deficiency, current allopurinol use, routine contraindications to MRI and pregnancy. Written informed consent was obtained from all participants. The study was approved by the South Central –Oxford C NHS Health Research Authority Ethics Committee 12/SC/0366.

Following endovascular aneurysm occlusion, all patients were managed according to a standardised clinical SAH protocol. This included nimodipine (either 60 mg 4 hourly or 20 mg 2 hourly depending on blood pressure) for 21 days following diagnosis of SAH. No patient demonstrated clinical or angiographic evidence of DCI or cerebral arterial vasoconstriction at the time of the study.

2.2. Study design

All patients successfully recruited to the study were randomised to receive an infusion of sodium nitrite at 10 mcg/kg/min or 0.9 % saline at the equivalent rate (0.12 ml/kg/h). Simple 1:1 non-stratified randomisation was performed via sequentially numbered opaque sealed envelopes prepared by an independent person, not involved in data collection and analysis.

Before the infusions were commenced all patients underwent baseline MRI (MRI 1) scanning within 92 hours of ictus. Study infusions were commenced within 1 hour of MRI 1 completion. All infusions were prepared by a suitably trained medical practitioner independent of the study. Infusions were delivered via a peripherally sited intravenous canula using a calibrated infusion pump. Both the patient and researchers were blinded to the allocation. All infusions were administered for 3 h before repeat MRI (MRI 2) was then performed with the infusions continuing to be administered throughout the duration of the scanning protocol.

2.3. Sodium nitrite

Sodium nitrite has been established as safe for long term use in human SAH [30] (4.45mcg/kg/min for 14 days). However, plasma nitrite levels achieved at such an infusion rate are below those identified in animal studies as maximally efficacious [31]. In healthy volunteers, doses of up to 110mcg/kg/min have been given safely, however, at high doses [32] and long infusions [33], side effects of decreased blood pressure and methaemoglobinemia become clinically significant. Pharmacokinetic data suggests that at an infusion of 10mcg/kg/min, plasma nitrite levels will plateau at around 2 hours. The infusion rate and duration were therefore chosen as a compromise between ensuring adequate steady state plasma nitrite levels and minimisation of any cardiovascular effect.

2.4. Clinical follow up

The diagnosis of delayed cerebral ischemia was made by the attending clinicians who were independent to the study. The definition of delayed cerebral ischemia was in line with the guidelines proposed by Vergouwen et al. [34], being, "*The occurrence of focal neurological impairment (such as hemiparesis, aphasia, apraxia, hemianopia, or neglect), or a decrease of at least 2 points on the Glasgow Coma Scale. This should last for at least 1 hour, is not apparent immediately after aneurysm occlusion, and cannot be attributed to other causes by means of clinical assessment, CT or MRI scanning of the brain, and appropriate laboratory studies*". Each patient was also assessed at discharge and at 3 months using the Glasgow outcome scale (GOS) [35].

2.5. Physiological monitoring

During the study, infusion oxygen saturations (SpO2), heart rate and non-invasive blood pressure (NIBP) were measured every 5 minutes for the first 15 minutes and then every 15 minutes (Dinamap Procare 300, GE Healthcare). In addition, methaemoglobin levels were assessed non-invasively by pulse co-oximetry (Masimo Rainbow, Switzerland).

During MRI, oxygen saturations (SpO2), heart rate and non-invasive blood pressure (NIBP) were measured every 15 minutes (Philips MR400). End tidal CO2 and O2 (KPa) were continuously monitored using disposable nasal cannulae and side stream infrared and optical sensors, respectively (AD Instruments). Two-point calibration was performed prior to each session using calibration gas (7 % O2, 5 % CO2, balance Nitrogen; Speciality Gases). All data was sampled at 100Hz on a Powerlab data acquisition interface (AD Instruments) and recorded for off line analysis following anti-aliasing filtering, with a low-pass frequency cut-off at 20 Hz.

2.6. MRI imaging protocol

A Siemens MAGNETOM 3T Verio scanner with a 12 channel head coil (Siemens Healthcare, Erlangen, Germany) located at the Oxford Acute Vascular Imaging Centre (AVIC) was used for all scans.

The Scanning protocol included the following sequences:

High resolution T1-weighted MPRAGE whole brain structural

scans for registration and tissues segmentation: 1.5 × 1.5 × 1.5 mm resolution; TR 1780 ms; TI 900 ms; TE 4.4 ms.

Time-of-flight MR neck angiogram, to facilitate vessel labelling: 1.5 min; 20 slices; 1.2 × 0.8 × 1.3 mm; TR 26 ms; TE 3.43 ms; flip angle 18 deg.

Multi-Post labelling delay (PLD) vessel-encoded pseudocontinuous arterial spin labeling (VEPCASL) perfusion-weighted imaging to measure changes in perfusion: 3.4 × 3.4 × 4.5 mm, field of view 220 mm; TR 4080 ms; TE 14 ms, echo planar imaging readout, 24 slices, background suppression with multiple post-labeling delays (0.25 s, 0.5 s, 0.75 s, 1 s, 1.25 s, 1.5 s). The vessel encoding protocol consisted of a 1.4 s pulse train cycling through eight different vessel-encodings: two non-selective (label and control), two left-right, two anterior-posterior and two diagonal. Two repetitions of these encodings were acquired for each PLD. The labelling plane was positioned approximately 8 cm below the circle of Willis, at the proximal V3 segment of the vertebral arteries. Calibration scans were acquired to allow absolute perfusion quantification using the same parameters as the VEPCASL, but without labelling or background suppression [28,36].

The structural MRIs were reviewed for clinical purposes by a consultant neuroradiologist and any abnormalities reported back to the clinical team looking after the patient.

2.7. Analysis

2.7.1. Physiological parameters

CO2 waveform data pre-processing was carried out using custom written MATLAB scripts (MATLAB R2018b, The MathWorks Inc., Natick, MA, 2000). The CO2 waveform was visually inspected for significant artefact and end tidal CO2 (ETCO2) values were calculated via waveform peak identification.

2.7.2. Structural pre-processing

T1 weighted image pre-processing was carried out using FSL Version 6.0.1 (FMRIB Software Library, Functional Magnetic Resonance Imaging of the Brain Centre, Department of Clinical Neurosciences, University of Oxford, Oxford, UK, http://www.fmrib.ox.ac.uk) [37]. In summary, this included visual inspection of the scans to check for gross artefact, brain extraction using BET and tissue segmentation and partial volume estimation using FAST.

2.7.3. Arterial spin labelling

Retrospective motion correction was applied using the MCFLIRT [37,38]. Calculation of the perfusion from each artery at each PLD was achieved using a maximum a posteriori approach to the general Bayesian framework for vessel-encoded data [36,39]. A kinetic model, incorporating a macrovascular component, was fitted to the data for each feeding artery, separately, to estimate perfusion, arterial cerebral blood volume (aCBV), arterial transit time and the associated variances

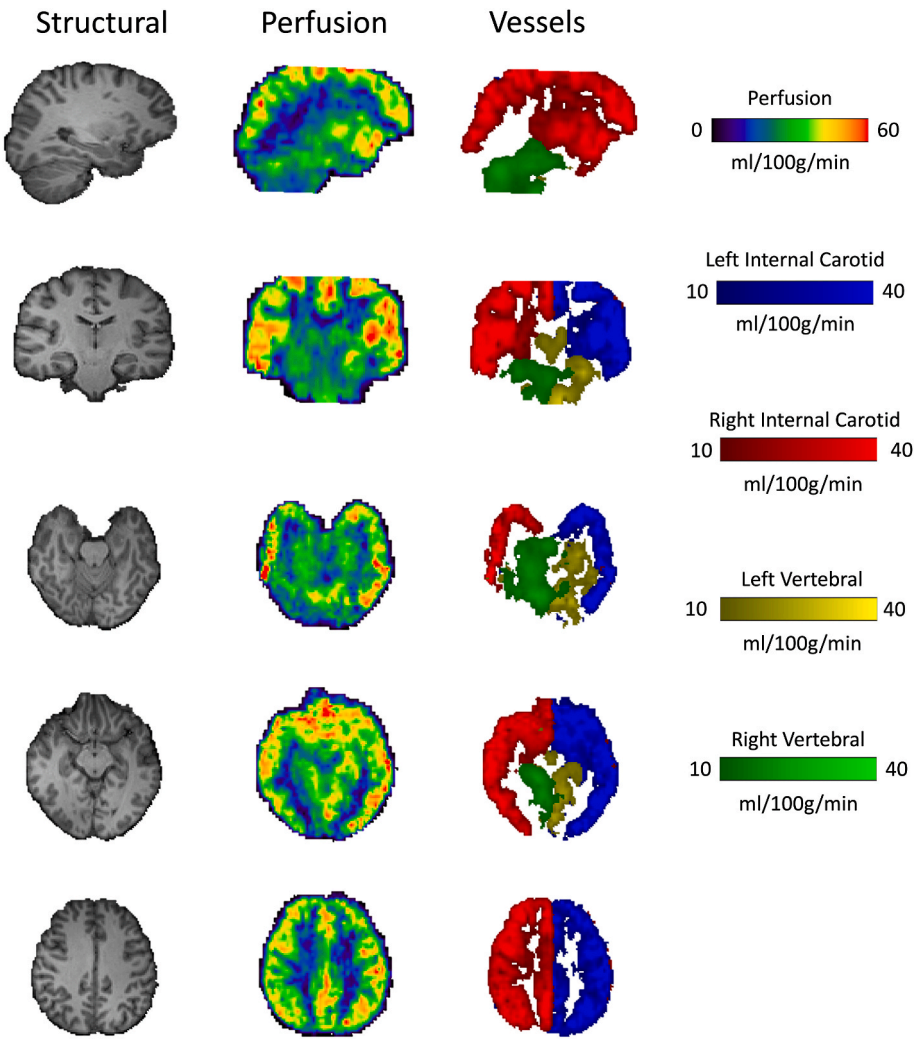

Fig. 1. Multi-PLD VEPCASL results for a single representative subject in subject T1 structural space demonstrating perfusion, and feeding artery distribution maps.

using a variational Bayes approach employing spatial priors [40–42]. Voxelwise calibration was performed to derive absolute parameter estimates. Fig. 1 demonstrates the perfusion and feeding artery distribution maps in structural space of a single representative subject at baseline.

Whole brain grey matter (GM) perfusion was calculated by taking the average across a GM mask created by a linear transform (FLIRT and BBR) of the GM partial volume map (derived from the T1-weighted image segmentation) into ASL space and thresholding at 0.5. Non-linear registration to the MNI-152 2 mm standard space via T1 weighted structural scans (BBR, FLIRT, FNIRT) was also performed to enable voxelwise statistical inference.

2.7.4. ASL kinetic model

The effects of sodium nitrite on the biophysics of the ASL signal must be accounted for to avoid systematic bias in the perfusion estimates. The quantification of perfusion from arterial spin labelling perfusion MRI is based upon the principles of tracer kinetics. The labelled blood water is treated as a tracer, which gives rise to a measured signal. As such, the longitudinal decay of the labelled blood water strongly influences the kinetic model. During analysis, blood T1 must be defined, and is often assumed to be the same for all individuals. However, the longitudinal decay of blood water is dependent on the biochemical and physiological composition of the blood itself. The administration of sodium nitrite is known to cause a small but significant increase in methaemoglobin. Methaemoglobin has a strong effect on blood longitudinal relaxation, introducing between session bias. To account for this confounding effect, blood water T1 was calculated on individual patient basis for each scan, using the approach set out by Li et al. [43] and methaemoglobin fraction determined from the non-invasive physiological measure taken during the study. For a detailed description see Supplementary Data.

2.7.5. Calibration

M0a calibration to derive absolute perfusion estimates was performed using a voxelwise approach. This has the additional benefit of accounting for transmit/receive field inhomogeneities and transverse relation effects at the voxel level. A CSF reference region approach was not used in this analysis, since SAH is associated with blood within the ventricular system and haemoglobin in varying states of breakdown will have a significant effect on the magnetisation estimate of CSF.

2.7.6. Statistical analysis

2.7.6.1. Whole brain ASL measures. To assess for the effect of sodium nitrite, statistical analysis of the whole brain ASL perfusion was carried out using R (R Foundation for Statistical Computing) [44] and the analysis package nlme (R package version 3.1–131) [45]. A two level mixed effects model was employed. Using a random intercept model with the ASL measure conditional on patient, allowed for within patient correlation due to repeated measures on each patient over time. The study arm allocation (placebo/sodium nitrite) and imaging time point (MRI 1/MRI 2) were included as fixed effects, in addition to confounding factors that may influence cerebrovascular haemodynamics (age, WFNS score, DCI, ETCO2, mean arterial pressure).

2.7.6.2. Voxelwise analysis. Voxelwise statistical inference was performed using the FMRIB Local Analysis of Mixed Effects (FLAME) algorithm [46]. This enabled the incorporation of the variance maps from each participant's ASL measures into the model. By doing so, the statistical maps are weighted by the reliability of the individual's data.

To test for the effect of sodium nitrite, the interaction between arm allocation and imaging time point was assessed using a repeated measure within subject ANOVA. Z statistic images were thresholded using clusters determined by $Z > 2.3$ and a (family-wise error (FWE) corrected) cluster significance threshold of $p < 0.05$.

2.7.6.3. Clinical data. Comparison of baseline demographic, clinical and physiological data was compared using Fishers exact test for categorical data, Mann-Whitney *U* test for unpaired ordinal and non-parametric continuous data, Wilcoxon test for paired ordinal and non-parametric continuous data and paired/unpaired t-tests for parametric continuous data.

3. Results

3.1. Clinical demographics

Between April 2016 and June 2018, 54 patients were screened for eligibility into the study. Of those that were eligible, 16 patients were recruited. A subset of these patients also underwent EEG assessment during the infusion sodium nitrite/saline placebo, the results of which are published in Luettich et al. [27] The mean time from ictus to the primary MRI scan was 66 hours (range 34–90 hours). All primary MRI scans were performed at the same time period during the day (between 9am and 11am).

All 16 patients who underwent MRI 1 received the nitrite/placebo infusion for 3 hours and underwent secondary MRI scanning (MRI 2). All secondary scans were performed at the same time period during the day (2pm–5pm). Inspection of the ASL data identified significant movement artefact in both the MRI 1 and MRI 2 scans in a single patient. This patient was excluded from subsequent analysis.

Fig. 2 is a flow sheet outlining recruitment into the study. Table 1 is a detailed breakdown of the demographics and clinical data for each patient recruited into the study.

3.2. Effect of sodium nitrite on cerebral haemodynamics during early brain injury

3.2.1. Randomisation

9 patients were randomised to saline placebo and 7 to sodium nitrite. The excluded patient, due to excessive movement artefact, was randomised to sodium nitrite. Therefore only 6 patients who received sodium nitrite were included in subsequent comparisons.

3.2.2. Clinical demographics

Table 2 shows a summary of the clinical demographics between patients included in the final analysis in both study arms. No significant differences were observed in baseline characteristics or clinical measures.

3.2.3. Physiological data

Physiological data recorded during the MRI 1 and MRI 2 scanning sessions for patients included in the final analysis in both study arms is presented in Table 3. During MRI 1 no significant differences in the physiological data were observed between nitrite and control arms. During MRI 2, as expected, methaemoglobin was significantly higher in nitrite group (0.99 (0.18) vs 3.13 (0.23), $p < 0.001$). Oxygen saturations, mean arterial pressure, heart rate, and end tidal CO2 were not statistically different between nitrite and control arms.

3.2.4. Whole brain average ASL results

The results of the linear mixed effects modelling of mean grey matter perfusion are as follows: Within study arm comparisons identified that, in patients randomised to the nitrite arm, mean perfusion significantly increased between MRI 1 and MRI 2 (baseline mean perfusion = 39.147 ml/100 g/min (SEM = 3.39) to infusion mean perfusion = 49.764 ml/100 g/min (SEM = 3.37); p value = 0.0025). In patients randomised to the placebo arm there was no change in mean perfusion between MRI 1 and MRI 2 (baseline mean perfusion = 41.783 ml/100 g/min (SEM = 2.75) to infusion mean perfusion = 40.732 ml/100 g/min (SEM = 2.75); p value = 0.6885).

Within MRI scan comparisons identified that there was no significant

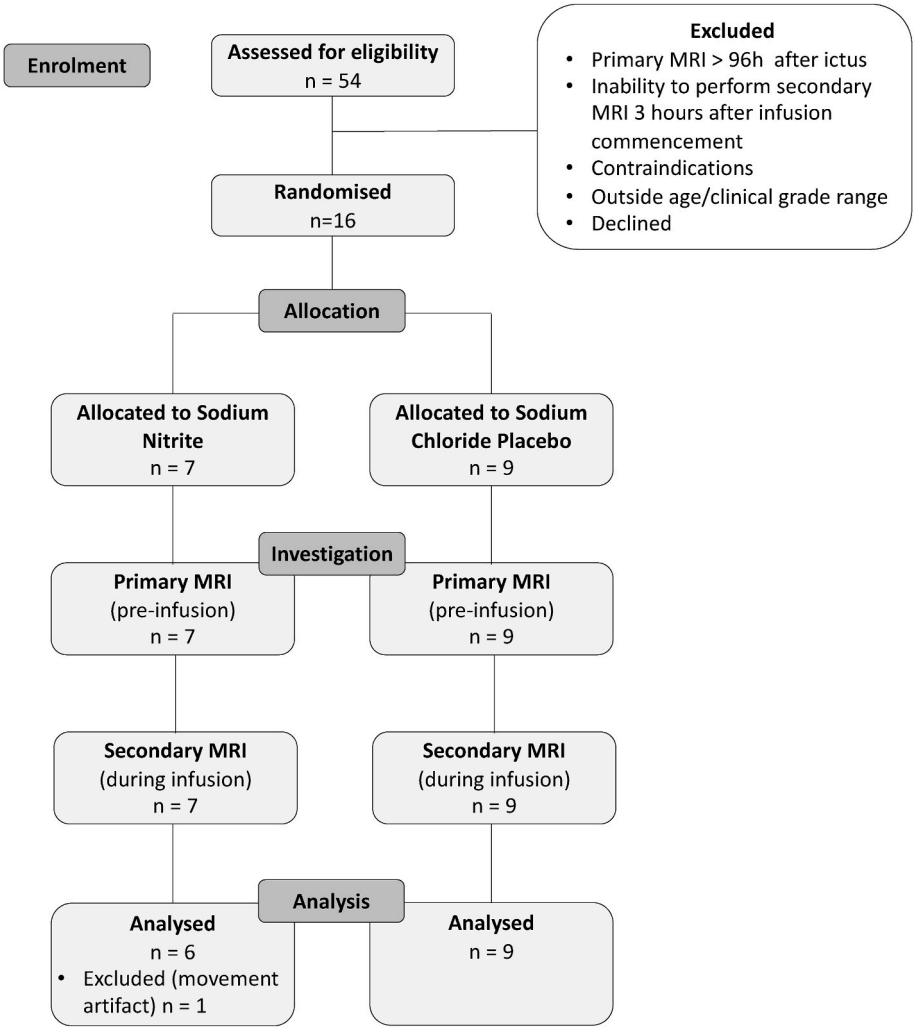

Fig. 2. Flowsheet of study recruitment.

Table 1
Demographics of all recruited patients. Abbreviations: Comm, communicating; A, Anterior; P, Posterior; ICA, Internal Carotid Artery; MCA, Middle Cerebral Artery; HTN, hypertension; IHD, ischemic heart disease; CSF, Cerebrospinal Fluid; EVD, External ventricular drain, LOS, length of stay; GOS, Glasgow outcome scale; DCI, delayed cerebral ischemia; WFNS, World Federation of Neurosurgeons.

Patient	Age (years)	Gender	Location of Aneurysm	HTN	IHD	WFNS Grade	Fisher Grade	CSF diversion	Discharge Destination	LOS (days)	GOS at Discharge	GOS at 3 mo	DCI	Allocation
1	51	Male	A. Comm	No	No	1	2	none	Home	8	5	5	No	Nitrite
2	51	Female	A. Comm	No	No	2	4	none	Home	15	5	5	No	Placebo
3	30	Male	Opthalmic	No	No	1	2	none	Home	14	5	5	No	Placebo
4	31	Female	A. Comm	No	No	1	3	none	Home	10	5	5	No	Nitrite (excluded)
5	61	Female	P. Comm	Yes	No	1	4	none	Home	12	5	5	No	Placebo
6	64	Female	Pericallosal	Yes	No	2	4	EVD	Hospital	18	3	5	No	Nitrite
7	49	Male	A. Comm	Yes	No	1	4	none	Home	10	5	5	No	Placebo
8	61	Male	A. Comm	No	No	1	4	none	Home	12	5	5	No	Nitrite
9	50	Female	P. Comm	Yes	No	1	2	none	Home	10	5	5	No	Placebo
10	45	Male	P. Comm	Yes	No	1	2	none	Home	11	5	5	No	Placebo
11	51	Female	P. Comm	No	No	2	4	none	Hospital	17	4	5	Yes	Placebo
12	52	Female	Superior cerebellar	No	No	1	1	none	Home	11	5	5	No	Placebo
13	64	Female	MCA	Yes	No	1	4	none	Home	10	5	5	Yes	Nitrite
14	36	Male	A. Comm	No	No	1	2	none	Home	8	5	5	No	Nitrite
15	42	Female	ICA	No	No	2	2	none	Home	9	5	5	No	Nitrite
16	29	Male	A. Comm	No	No	1	3	none	Home	10	5	5	No	Placebo

Table 2
Placebo vs Nitrite Patient Demographics included in final analysis.

	Nitrite	Placebo	p-value
Overall Demographics			
n	6	9	
Age (mean/range)	53 (36–64)	46.4 (29–61)	0.28
Gender (M:F)	3:3	4:5	>0.99
WFNS			
1	4	7	>0.99
2	2	2	
Fisher Grade			
1	0	1	>0.99
2	0	3	
3	3	1	
4	3	4	
Aneurysm Location (%)			
Anterior Circulation	4	4	0.08
Middle Cerebral	1	0	
Internal Cartotid	1	0	
Vertebral Artery	0	0	
Posterior Circulation	0	5	
Complications			
DCI	1	2	

Table 3
Physiological data for both MRI time points in patients included in final analysis for both study arms.

	MRI 1			MRI 2		
	Placebo	Nitrite	p-value	Placebo	Nitrite	p value
MAP (mmHg)	91.6 (11.7)	91.8 (8.2)	0.97	90.5 (10.1)	85.4 (9.2)	0.33
Heart Rate (bpm)	61 (8.2)	56.2 (6.3)	0.33	61 (7.5)	58 (14)	0.6
SpO2 (%)	97 (1)	97.1 (2.6)	0.54	97 (2)	96 (1.4)	0.9
End Tidal CO2 (kPa)	3.9 (0.14)	3.96 (0.12)	0.43	3.9 (0.3)	4 (0.2)	0.5
MetHb	0.93 (0.25)	0.97 (0.33)	0.83	0.99 (0.18)	3.13 (0.23)	**<0.001**

difference in MRI 1 mean perfusion between patients randomised to placebo or nitrite (p value = 0.549). Whereas, during MRI 2 there was a significant difference in mean perfusion between patients receiving sodium nitrite and those receiving the placebo (p value = 0.047). These results are illustrated in Fig. 3. Normality and homoscedasticity in the residuals was assessed by examining the qqnorm plot of the model residuals (Fig. 4a) and standardised residuals vs. fitted residuals for the model (Fig. 4b) respectively. These demonstrated that the model is a good fit for the data. There were no significant effects of Age, WFNS grade, MAP and etCO2 level on the mean perfusion.

3.2.5. Voxelwise analysis

Fig. 5a shows the z-statistics depicting the spatial regions, with a significant positive interaction effect between arm allocation and imaging time point (Scan 2 Nitrite – Scan 1 Nitrite) > (Scan 2 Placebo – Scan 1 Placebo). Significant clusters are visible in the caudate, putamen, frontal pole, precuneous cortex, insular cortex, paracentral lobule, precentral, middle and inferior frontal gyri, and anterior and posterior cingulate gyri.

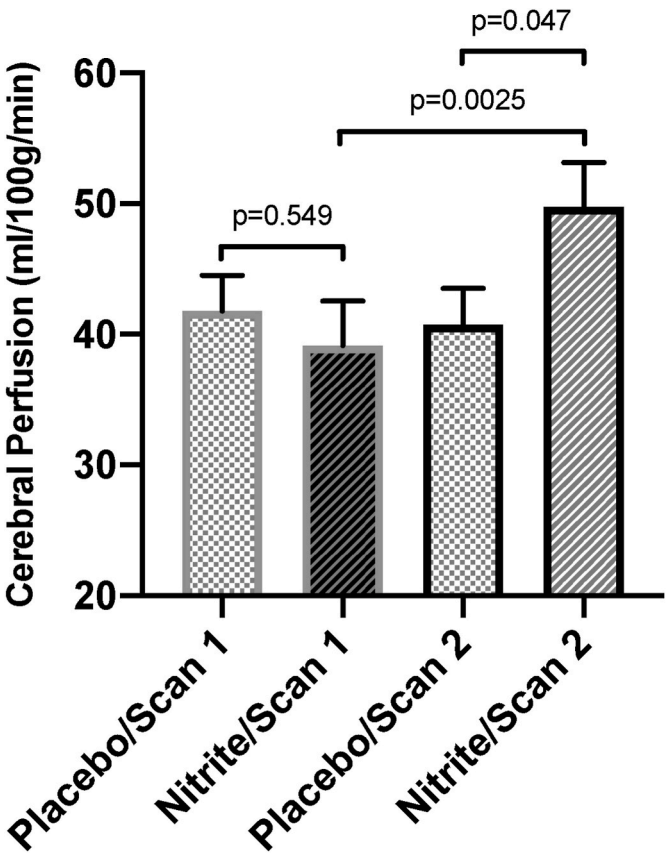

Fig. 3. Bar chart of mean cerebral perfusion, for the different conditions. A significant increase in perfusion in patients following sodium nitrite is visible. Perfusion is also significantly larger in patients that received sodium nitrite that those who received placebo during the second scan. There is no difference between infusion groups at baseline. Bars represent standard error of the mean (SEM).

4. Discussion

4.1. Main findings

The aim of this study was to test the hypothesis that administration of an exogenous NO donor, in the form of sodium nitrite, would increase cerebral perfusion during early brain injury following subarachnoid haemorrhage. Administration of sodium nitrite was associated with a significant increase in average grey matter cerebral perfusion, whereas in patients that received a placebo infusion perfusion remained unchanged. The spatial distribution of increased cerebral perfusion correlates with regions of the brain known to exhibit enhanced vulnerability to injury.

4.2. The role of nitric oxide pathway dysfunction during early brain injury

Early brain injury and the subsequent development of DCI have been shown to be associated with impaired cerebral autoregulation and blood flow [4–19]. We have previously reported that sodium nitrite administration during EBI improves EEG makers of ischemia and normalises cerebral blood flow haemodynamics [25–27]. The increase in mean grey matter perfusion observed within this study, when viewed in combination with our previous findings, suggests that sodium nitrite administration acts to improve cerebrovascular function and tissue perfusion. These findings add significant weight to the role of reduced NO bioavailability in the pathophysiology of EBI and potentially the subsequent development of DCI.

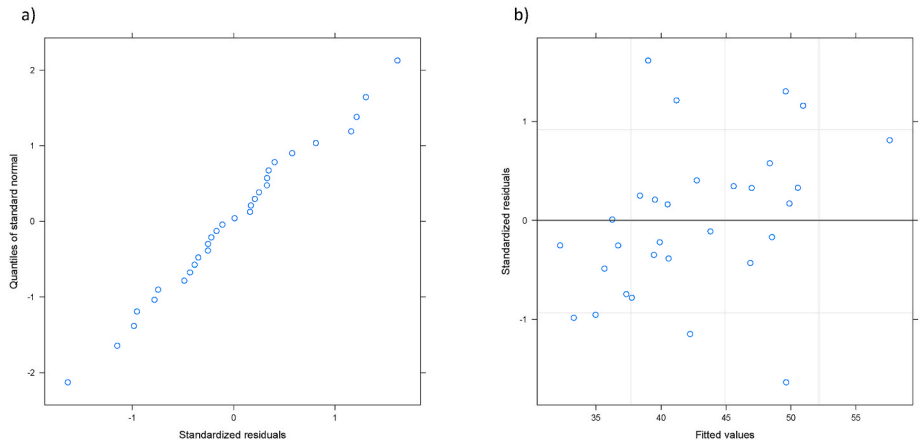

Fig. 4. Diagnostic plots to show the a) normality of the residuals in the linear mixed effects model and b) the fitted model is unbiased and homoscedastic. These plots demonstrate that the model is a good fit for the data.

4.3. Regional perfusion changes following sodium nitrite administration

To date, studies assessing perfusion in the immediate days following aneurysmal rupture, have done so using predefined regions of interest, normally based on anatomical vascular territories from which global values are derived [19,47–54]. Little attention has been paid to specific patterns of regional perfusion. As such, direct comparison of our findings with other studies in this field is not possible. It is therefore difficult to determine if the increase in perfusion identified following nitrite administration is localised to cerebral regions that exhibit impaired perfusion during EBI.

However, the regions identified in our study with increased perfusion following sodium nitrite administration correlate with those known to exhibit enhance vulnerability to injury. The increase in perfusion in the caudate, putamen, insular cortex, paracentral lobule, precentral, middle and inferior frontal gyri, corresponds with those identified by Payabvash et al., as demonstrating higher levels of ischaemic vulnerability to hypoperfusion [55]. In that study, the percent infarction increase per unit relative perfusion reduction was determined for different brain regions in patients having acutely suffered from an ischemic stroke. Vulnerable regions were defined as those that demonstrated higher infarct burden per unit reduction in relative perfusion. We also observed a significant increase in perfusion in the frontal pole, anterior and posterior cingulate gyri, and precuneous cortex. These regions demonstrate high levels vulnerability to diffuse axonal injury following traumatic brain injury. The high density of connections that pass through these midline areas are believed to render these regions especially susceptible to shear/strain injury [56–58].

It has been well described in animal studies, that the immediate period following aneurysmal rupture is associated with a profound mechanical and ischaemic insult [59]. It is, therefore, reassuring that nitrite administration increases cerebral perfusion in cortical regions where we may expect to observe the greatest injury burden.

4.4. Sodium nitrite site of pharmacodynamic action

An increase in perfusion following sodium nitrite administration in cortical regions with the greatest injury burden corresponds with the known biochemistry of nitrite [60]. Nitrite is reduced to bioactive NO through acidification or via reaction by a number of proteins possessing nitrite reductase activity. Critically, the reduction of nitrite by the reductases is enhanced in conditions of hypoxia or acidosis. Neuroglobin, present in the cells of all mammalian brains, contains a hexa-coordinated haeme group that is converted to a penta-coordinated form during periods of oxidative stress. In this form, it readily reduces nitrate to nitric oxide. Thus, regions with higher levels of injury burden are more likely to reduce nitrite to NO and exhibit increased perfusion. This is supported by the recent finding of Franko et al. who demonstrated no effect on EEG measures or transcranial Doppler derived cerebral blood flow during the administration of sodium nitrite in healthy volunteers [61]. Cerebral acidosis or hypoxia would not be expected in this group, suggesting that nitrite is not reduced to NO in normal brain tissue.

The reduction of nitrite to NO at parenchymal level would support the hypothesis that, during EBI, sodium nitrite has it pharmacodynamic site of action on the cerebral microvasculature. There is increasing preclinical and clinical evidence to suggest that microvascular dysfunction plays a critical role in early brain injury following SAH [48–50,62–65]. Several pathological processes have been proposed to induce microvascular dysfunction following SAH. Critically, NO appears to play a significant role in this process. Reduced NO bioavailability following SAH has been shown to result in unopposed vascular myogenic reactivity [66,67], microthrombus formation secondary to increased P-selectin levels [68,69] and pericytes hypercontractile [70].

This observation is also supported by murine models of subarachnoid haemorrhage, which have demonstrated that inhaled nitric oxide administration reduced early microvascular dysfunction [71]. Inhaled nitric oxide is believed to confer its cerebral action through the formation of bioactive nitric oxide carriers, such as nitrite, in the lung [72,73]. As such, inhaled nitric oxide demonstrates the same selectivity to cerebral regions with higher levels of injury burden [74,75]. Inhaled nitric oxide has subsequently been examined in patients with delayed cerebral ischemia following SAH [76]. In this study, multimodal assessment of cerebrovascular function was assessed in patients with delayed cerebral ischemia during inhaled nitric oxide treatment. A consistent increase in cerebral tissue oxygen partial pressure was demonstrated, whereas macrovascular changes assessed using transcranial doppler and digital subtraction angiography were less consistently observed and less pronounced. It was suggested by the authors that these findings support evidence from murine models that inhaled nitric oxide predominantly exerts its effects at the microvascular level.

These findings would appear at odds with the pre-clinical findings of both Pluta et al. and Fathi et al. Utilising primate autologous blood clot models of SAH, cerebral large vessel constriction was demonstrated to be reversed or prevented by the administration of sodium nitrite [77,78]. Given the known spatial correlation between cerebral blood load and the development of large vessel constriction, it was proposed that nitrite reduction by deoxyhaemoglobin within the clot was the basis of its action. However, several key differences exist between our study and those discussed above. Pluta et al. and Fathi et al. sought to examine the effect of nitrite administration on large vessel constriction associated with DCI. Thus, they performed cerebral angiography on day 7 after clot

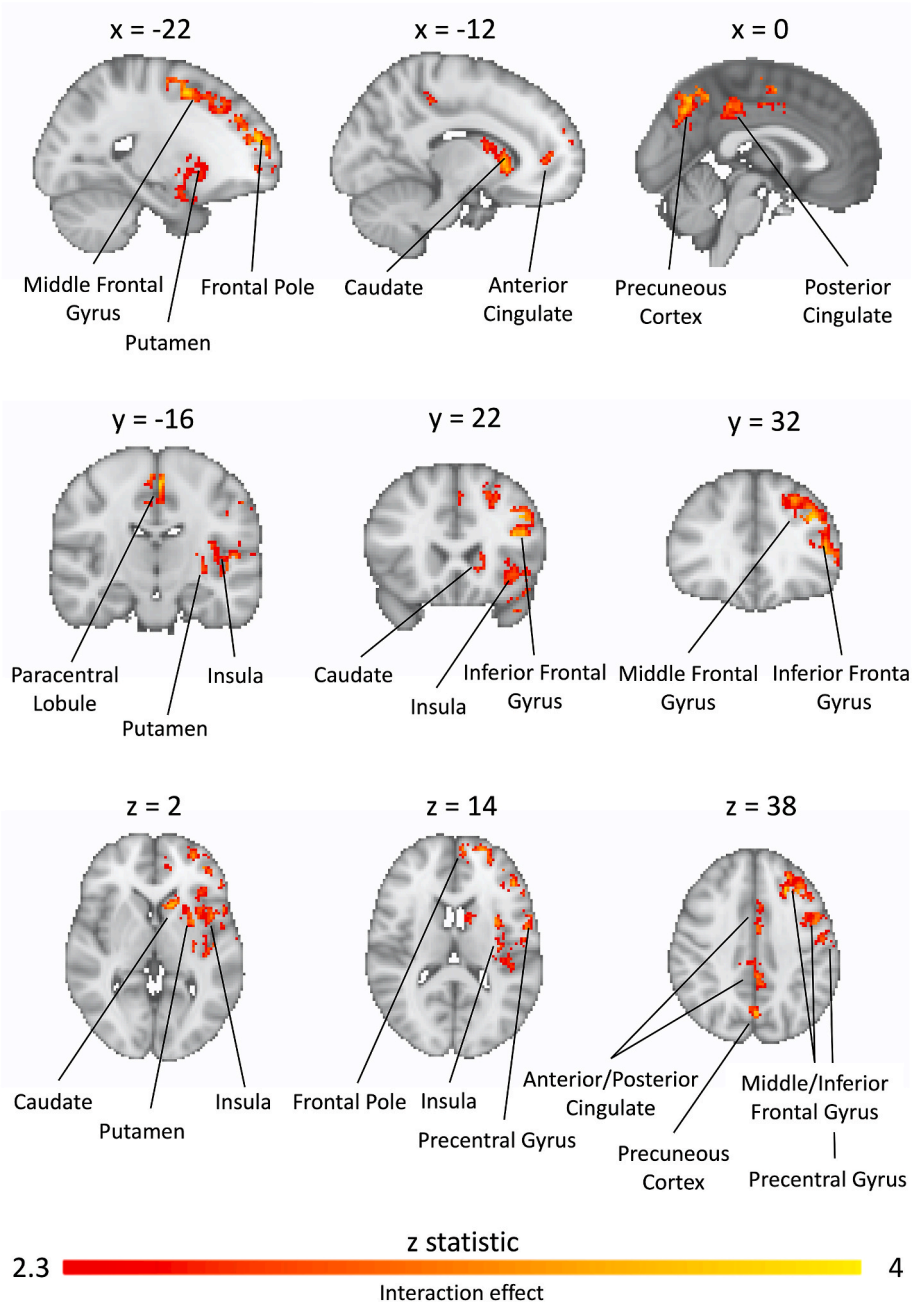

Fig. 5. Standard space (MNI 2 × 2 × 2 mm) representation of mixed effects repeated measures interaction analysis (FLAME) of perfusion data incorporating individual subject variance maps. Demonstrates interaction between infusion arm and scan time point ((Scan 2 Nitrite – Scan 1 Nitrite) > (Scan 2 Placebo – Scan 1 Placebo)). Statistical maps consist of a colour-rendered statistical map superimposed on a standard brain, and significant regions are displayed with a threshold Z > 2.3, with a cluster probability threshold of $p < 0.05$ (corrected for multiple comparisons).

placement, during the DCI window, when large vessel constriction is expected to occur. Our study, sought to determine the role NO pathway disfunction plays in EBI. Assessment was, therefore, performed during the EBI period (first 72 hours after aneurysmal rupture), before we would not expect to observe large vessel constriction. Furthermore, from a methodological perspective, autologous blood clot models of SAH, whilst ideal for examining cerebral vasospasm, do not induce the profound early pathophysiological changes associated with aneurysmal rupture [59]. Therefore, even within this period, the observable action of nitrite administration will be intrinsically limited to the effects on clot induced large vessel constriction.

4.5. Sodium nitrite and DCI

One of the key findings of Garry et al. [25]was the differential EEG response following sodium nitrite administration between patients that subsequently developed DCI and those that did not. The differential response observed was proposed to indicate the severity of the underlying cerebral injury and therefore likelihood of progressing to develop DCI. Unfortunately, we were unable to make any meaningful comparisons, as only one patient who received sodium nitrite subsequently developed DCI.

4.6. Limitations

The small sample size represents the primary limitation of this study. However, this represents the first study to investigate, in detail, the cerebral perfusion response to exogenous NO administration during EBI using ASL. In doing so, it provides valuable insight into the potential role of NO in the pathophysiology of EBI and the possible role of state-of-the-art VEPCASL in the serial assessment of cerebral perfusion following SAH.

It is also reassuring that the increase in cerebral perfusion following sodium nitrite administration observed within this study is in line with the EEG and TCD findings of our previous studies.

To account for the effects of methaemoglobin on the longitudinal relaxation of blood water, individual adjustments to the ASL kinetic model T1 blood value were required. As expected, the adjusted T1 blood values incorporating the effects of methemoglobinemia were significantly shorter. Inherently this will result in an increase in estimated cerebral perfusion. Blood methaemoglobin levels were measured non-invasively, the group average methaemoglobin level in the nitrite group was significantly large than the placebo group (3.13 vs 0.99 %). Given the reported precision of the Massimo rainbow system of 0.89 % [79], there may have been a systematic overestimation of methaemoglobin levels. Furthermore, we could only identify one model to estimate the effects of methaemoglobin at 3T. As such, any inaccuracies in this model may have resulted in an overestimation of the T1 shortening effect. However, if there was a systematic overestimation of the T1 shortening effect of methaemoglobin, we would expect to observe a non-specific global increase in cerebral perfusion. Our findings demonstrate localised changes in brain regions known to exhibit enhance vulnerability, indicating that T1 estimation does not have a dominant effect.

5. Conclusion

We have demonstrated that pharmacological manipulation of *in vivo* NO levels in patients with low grade SAH results in increased cerebral perfusion in regions of the brain known to exhibit enhanced vulnerability to injury. These findings suggest that reduced NO bioavailability plays a critical role in the pathophysiology of EBI, and supports future clinical trials of sodium nitrite treatment to prevent the development of DCI following SAH.

Funding

This work was supported by the Neuro Anaesthesia and Critical Care Society (WKRO-2015-0080) and the National Institute for Health Research (NIHR) Biomedical Research Centre (BRC) based at Oxford University Hospitals NHS Trust and The University of Oxford.

Statements and declarations

Drs. Ezra and Pattinson are named as coinventors on a provisional EU patent application titled “Use of cerebral nitric oxide donors in the assessment of the extent of brain dysfunction following injury.”

CRediT authorship contribution statement

Martyn Ezra: Writing – review & editing, Writing – original draft, Methodology, Investigation, Funding acquisition, Formal analysis, Data curation, Conceptualization. **Edit Franko:** Writing – review & editing, Investigation, Data curation. **Desiree B. Spronk:** Writing – review & editing, Investigation, Data curation. **Catherine Lamb:** Writing – review & editing, Investigation, Data curation. **Thomas W. Okell:** Writing – review & editing, Software, Formal analysis. **Kyle TS. Pattinson:** Writing – review & editing, Supervision, Methodology, Funding acquisition, Conceptualization.

Data availability

Data will be made available on request.

Appendix A. Supplementary data

Supplementary data to this article can be found online at https://doi.org/10.1016/j.niox.2024.10.003.

Highlights the importance of the NO pathway following subarachnoid haemorrhage.

References

[1] C.E. Lovelock, G.J.E. Rinkel, P.M. Rothwell, Time trends in outcome of subarachnoid hemorrhage: population-based study and systematic review, Neurol. Now. 74 (19) (May 2010) 1494–1501, https://doi.org/10.1212/WNL.0b013e3181dd42b3.

[2] O. Rivero-Arias, A. Gray, J. Wolstenholme, Burden of disease and costs of aneurysmal subarachnoid haemorrhage (aSAH) in the United Kingdom, Cost Eff. Resour. Allocation 8 (1) (Apr. 2010) 6, https://doi.org/10.1186/1478-7547-8-6.

[3] M.J. Rowland, G. Hadjipavlou, M. Kelly, J. Westbrook, K.T.S. Pattinson, Delayed cerebral ischaemia after subarachnoid haemorrhage: looking beyond vasospasm, Br. J. Anaesth. 109 (3) (Sep. 2012) 315–329, https://doi.org/10.1093/bja/aes264.

[4] K.P. Budohoski, et al., Impairment of cerebral autoregulation predicts delayed cerebral ischemia after subarachnoid hemorrhage: a prospective observational study, Stroke 43 (12) (Dec. 2012) 3230–3237, https://doi.org/10.1161/STROKEAHA.112.669788.

[5] K.P. Budohoski, et al., Bilateral failure of cerebral autoregulation is related to unfavorable outcome after subarachnoid hemorrhage, Neurocritical Care 22 (1) (Feb. 2015) 65–73, https://doi.org/10.1007/s12028-014-0032-6.

[6] L. Calviere, et al., Prediction of delayed cerebral ischemia after subarachnoid hemorrhage using cerebral blood flow velocities and cerebral autoregulation assessment, Neurocritical Care 23 (2) (Oct. 2015) 253–258, https://doi.org/10.1007/s12028-015-0125-x.

[7] J. Fontana, H. Wenz, K. Schmieder, M. Barth, Impairment of dynamic pressure autoregulation precedes clinical deterioration after aneurysmal subarachnoid hemorrhage, J. Neuroimaging 26 (3) (May 2016) 339–345, https://doi.org/10.1111/jon.12295.

[8] J.M.K. Lam, P. Smielewski, M. Czosnyka, J.D. Pickard, P.J. Kirkpatrick, Predicting delayed ischemic deficits after aneurysmal subarachnoid hemorrhage using a transient hyperemic response test of cerebral autoregulation, Neurosurgery 47 (4) (Oct. 2000) 819–826, https://doi.org/10.1097/00006123-200010000-00004.

[9] E.W. Lang, R.R. Diehl, H.M. Mehdorn, Cerebral autoregulation testing after aneurysmal subarachnoid hemorrhage: the phase relationship between arterial blood pressure and cerebral blood flow velocity, Crit. Care Med. 29 (1) (Jan. 2001) 158–163, https://doi.org/10.1097/00003246-200101000-00031.

[10] F. Otite, et al., Impaired Cerebral autoregulation is associated with vasospasm and delayed cerebral ischemia in subarachnoid hemorrhage, Stroke 45 (3) (Mar. 2014) 677–682, https://doi.org/10.1161/STROKEAHA.113.002630.

[11] K. Schmieder, et al., Dynamic cerebral autoregulation in patients with ruptured and unruptured aneurysms after induction of general anesthesia, Zentralbl. Neurochir. 67 (2) (May 2006) 81–87, https://doi.org/10.1055/s-2006-933374.

[12] M. Soehle, M. Czosnyka, J.D. Pickard, P.J. Kirkpatrick, Continuous assessment of cerebral autoregulation in subarachnoid hemorrhage, Anesth. Analg. 98 (4) (Apr. 2004) 1133–1139, https://doi.org/10.1213/01.ANE.0000111101.41190.99.

[13] Y. Duan, et al., Computed tomography perfusion deficits during the baseline period in aneurysmal subarachnoid hemorrhage are predictive of delayed cerebral ischemia, J. Stroke Cerebrovasc. Dis. 26 (1) (Jan. 2017) 162–168, https://doi.org/10.1016/J.JSTROKECEREBROVASDIS.2016.09.004.

[14] H. Sun, J. Ma, Y. Liu, C. You, CT perfusion for identification of patients at risk for delayed cerebral ischemia during the acute phase after aneurysmal subarachnoid hemorrhage: a meta-analysis, Neurol. India 67 (5) (Sep. 2019) 1235–1239, https://doi.org/10.4103/0028-3886.271235.

[15] D. Starnoni, et al., Early perfusion computed tomography scan for prediction of vasospasm and delayed cerebral ischemia after aneurysmal subarachnoid hemorrhage, World Neurosurg. 130 (Oct. 2019) e743–e752, https://doi.org/10.1016/J.WNEU.2019.06.213.

[16] V. Malinova, K. Dolatowski, P. Schramm, O. Moerer, V. Rohde, D. Mielke, Early whole-brain CT perfusion for detection of patients at risk for delayed cerebral ischemia after subarachnoid hemorrhage, J. Neurosurg. 125 (1) (Jul. 2016) 128–136, https://doi.org/10.3171/2015.6.JNS15720.

[17] C. Rodriguez-Régent, et al., Early quantitative CT perfusion parameters variation for prediction of delayed cerebral ischemia following aneurysmal subarachnoid hemorrhage, Eur. Radiol. 26 (9) (Sep. 2016) 2956–2963, https://doi.org/10.1007/S00330-015-4135-Z.

[18] L. Dong, Y. Zhou, M. Wang, C. Yang, Q. Yuan, X. Fang, Whole-brain CT perfusion on admission predicts delayed cerebral ischemia following aneurysmal subarachnoid hemorrhage, Eur. J. Radiol. 116 (Jul. 2019) 165–173, https://doi.org/10.1016/J.EJRAD.2019.05.008.

[19] A. Lagares, et al., Acute perfusion changes after spontaneous SAH: a perfusion CT study, Acta Neurochir. 154 (3) (Mar. 2012) 405–412, https://doi.org/10.1007/s00701-011-1267-z.

[20] P.S. Garry, M. Ezra, M.J. Rowland, J. Westbrook, K.T.S. Pattinson, "The Role of the Nitric Oxide Pathway in Brain Injury and its Treatment - from Bench to Bedside,", Jan. 2015, https://doi.org/10.1016/j.expneurol.2014.10.017.
[21] M. Suzuki, et al., Increased levels of nitrite/nitrate in the cerebrospinal fluid of patients with subarachnoid hemorrhage, Neurosurg. Rev. 22 (2–3) (Oct. 1999) 96–98, https://doi.org/10.1007/s101430050038.
[22] C.S. Jung, et al., Association of an endogenous inhibitor of nitric oxide synthase with cerebral vasospasm in patients with aneurysmal subarachnoid hemorrhage, J. Neurosurg. 107 (5) (2007) 945–950, https://doi.org/10.3171/JNS-07/11/0945.
[23] K. Rejdak, et al., Cerebrospinal fluid nitrite/nitrate correlated with oxyhemoglobin and outcome in patients with subarachnoid hemorrhage, J. Neurol. Sci. 219 (1–2) (Apr. 2004) 71–76, https://doi.org/10.1016/j.jns.2003.12.011.
[24] A. Woszczyk, W. Deinsberger, D.-K. Böker, Nitric oxide metabolites in cisternal CSF correlate with cerebral vasospasm in patients with a subarachnoid haemorrhage, Acta Neurochir. 145 (4) (Apr. 2003) 257–263, https://doi.org/10.1007/s00701-003-0004-7. ; discussion 263-4.
[25] P.S. Garry, et al., Electroencephalographic response to sodium nitrite may predict delayed cerebral ischemia after severe subarachnoid hemorrhage, Crit. Care Med. 44 (11) (Nov. 2016) e1067–e1073, https://doi.org/10.1097/CCM.0000000000001950.
[26] M. Ezra, P. Garry, M.J. Rowland, G.D. Mitsis, K.T. Pattinson, Phase dynamics of cerebral blood flow in subarachnoid haemorrhage in response to sodium nitrite infusion, Nitric Oxide 106 (Jan. 2021) 55–65, https://doi.org/10.1016/J.NIOX.2020.10.004.
[27] A. Luettich, et al., Beneficial effect of sodium nitrite on EEG ischaemic markers in patients with subarachnoid haemorrhage, Transl. Stroke Res. (2021), https://doi.org/10.1007/S12975-021-00939-9.
[28] T.W. Okell, M.A. Chappell, M.E. Kelly, P. Jezzard, Cerebral blood flow quantification using vessel-encoded arterial spin labeling, J. Cerebr. Blood Flow Metabol. 33 (11) (Nov. 2013) 1716–1724, https://doi.org/10.1038/jcbfm.2013.129.
[29] M. Labriffe, A. Ter Minassian, A. Pasco-Papon, S. N'Guyen, C. Aubé, Feasibility and validity of monitoring subarachnoid hemorrhage by a noninvasive MRI imaging perfusion technique: pulsed Arterial Spin Labeling (PASL), J. Neuroradiol. 42 (6) (Dec. 2015) 358–367, https://doi.org/10.1016/j.neurad.2015.04.001.
[30] E.H. Oldfield, et al., Safety and pharmacokinetics of sodium nitrite in patients with subarachnoid hemorrhage: a Phase IIA study, J. Neurosurg. 119 (3) (Sep. 2013) 634–641, https://doi.org/10.3171/2013.3.JNS13266.
[31] S. Shiva, et al., Nitrite augments tolerance to ischemia/reperfusion injury via the modulation of mitochondrial electron transfer, J. Exp. Med. 204 (9) (Sep. 2007) 2089–2102, https://doi.org/10.1084/jem.20070198.
[32] A. Dejam, et al., Nitrite infusion in humans and nonhuman primates: endocrine effects, pharmacokinetics, and tolerance formation, Circulation 116 (16) (Oct. 2007) 1821–1831, https://doi.org/10.1161/CIRCULATIONAHA.107.712133.
[33] R.M. Pluta, et al., Safety and feasibility of long-term intravenous sodium nitrite infusion in healthy volunteers, PLoS One 6 (1) (Jan. 2011) e14504, https://doi.org/10.1371/journal.pone.0014504.
[34] M.D.I. Vergouwen, et al., Definition of delayed cerebral ischemia after aneurysmal subarachnoid hemorrhage as an outcome event in clinical trials and observational studies: proposal of a multidisciplinary research group, J. cerebral circul. 41 (10) (Oct. 2010) 2391–2395, https://doi.org/10.1161/STROKEAHA.110.589275.
[35] B. Jennett, M. Bond, Assessment of outcome after severe brain damage, Lancet 1 (7905) (Mar. 1975) 480–484, https://doi.org/10.1016/s0140-6736(75)92830-5.
[36] M.A. Chappell, T.W. Okell, P. Jezzard, M.W. Woolrich, A general framework for the analysis of vessel encoded arterial spin labeling for vascular territory mapping, Magn. Reson. Med. 64 (5) (Nov. 2010) 1529–1539, https://doi.org/10.1002/mrm.22524.
[37] M. Jenkinson, C.F. Beckmann, T.E.J. Behrens, M.W. Woolrich, S.M. Smith, Fsl, Neuroimage 62 (2) (Aug. 2012) 782–790, https://doi.org/10.1016/j.neuroimage.2011.09.015.
[38] M. Jenkinson, P. Bannister, M. Brady, S. Smith, Improved optimization for the robust and accurate linear registration and motion correction of brain images, Neuroimage 17 (2) (Oct. 2002) 825–841, https://doi.org/10.1006/NIMG.2002.1132.
[39] M.A. Chappell, T.W. Okell, S.J. Payne, P. Jezzard, M.W. Woolrich, A fast analysis method for non-invasive imaging of blood flow in individual cerebral arteries using vessel-encoded arterial spin labelling angiography, Med. Image Anal. 16 (4) (May 2012) 831–839, https://doi.org/10.1016/j.media.2011.12.004.
[40] R.B. Buxton, L.R. Frank, E.C. Wong, B. Siewert, S. Warach, R.R. Edelman, A general kinetic model for quantitative perfusion imaging with arterial spin labeling, Magn. Reson. Med. 40 (3) (Sep. 1998) 383–396, https://doi.org/10.1002/mrm.1910400308.
[41] M.A. Chappell, A.R. Groves, B. Whitcher, M.W. Woolrich, Variational bayesian inference for a nonlinear forward model, IEEE Trans. Signal Process. 57 (1) (Jan. 2009) 223–236, https://doi.org/10.1109/TSP.2008.2005752.
[42] A.R. Groves, M.A. Chappell, M.W. Woolrich, Combined spatial and non-spatial prior for inference on MRI time-series, Neuroimage 45 (3) (Apr. 2009) 795–809, https://doi.org/10.1016/j.neuroimage.2008.12.027.
[43] W. Li, K. Grgac, A. Huang, N. Yadav, Q. Qin, P.C.M. van Zijl, Quantitative theory for the longitudinal relaxation time of blood water, Magn. Reson. Med. 76 (1) (Jul. 2016) 270–281, https://doi.org/10.1002/mrm.25875.
[44] R Core Team, Radiokhimiya: Lang Environ. Statist. Compu. (2017). Vienna, Austria. [Online]. Available: https://www.r-project.org/.
[45] J. Pinheiro, D. Bates, S. DebRoy, D. Sarkar, R Core Team, {nlme}: linear and nonlinear mixed effects models [Online]. Available: https://cran.r-project.org/package=nlme, 2017.
[46] M.W. Woolrich, T.E.J. Behrens, C.F. Beckmann, M. Jenkinson, S.M. Smith, Multilevel linear modelling for FMRI group analysis using Bayesian inference, Neuroimage 21 (4) (Apr. 2004) 1732–1747, https://doi.org/10.1016/j.neuroimage.2003.12.023.
[47] K. Aoyama, et al., Detection of symptomatic vasospasm after subarachnoid haemorrhage: initial findings from single time-point and serial measurements with arterial spin labelling, Eur. Radiol. 22 (11) (Nov. 2012) 2382–2391, https://doi.org/10.1007/s00330-012-2511-5.
[48] I.M.C. Huenges Wajer, et al., CT perfusion on admission and cognitive functioning 3 months after aneurysmal subarachnoid haemorrhage, J. Neurol. 262 (3) (Mar. 2015) 623–628, https://doi.org/10.1007/s00415-014-7601-7.
[49] P.S. Minhas, et al., Positron emission tomographic cerebral perfusion disturbances and transcranial Doppler findings among patients with neurological deterioration after subarachnoid hemorrhage, Neurosurgery 52 (5) (2003) 1017–1022. ; discussion 1022-4, May , Accessed: Jul. 15, 2019. [Online]. Available: http://www.ncbi.nlm.nih.gov/pubmed/12699542.
[50] J.W. Dankbaar, et al., Diagnostic threshold values of cerebral perfusion measured with computed tomography for delayed cerebral ischemia after aneurysmal subarachnoid hemorrhage, Stroke 41 (9) (Sep. 2010) 1927–1932, https://doi.org/10.1161/STROKEAHA.109.574392.
[51] I. van der Schaaf, M.J. Wermer, Y. van der Graaf, R.G. Hoff, G.J.E. Rinkel, B. K. Velthuis, CT after subarachnoid hemorrhage: relation of cerebral perfusion to delayed cerebral ischemia, Neurol. Now. 66 (10) (May 2006) 1533–1538, https://doi.org/10.1212/01.wnl.0000216272.67895.d3.
[52] M. Rijsdijk, I.C. van der Schaaf, B.K. Velthuis, M.J. Wermer, G.J.E. Rinkel, Global and focal cerebral perfusion after aneurysmal subarachnoid hemorrhage in relation with delayed cerebral ischemia, Neuroradiology 50 (9) (Sep. 2008) 813–820, https://doi.org/10.1007/s00234-008-0416-4.
[53] P.C. Sanelli, et al., Evaluating CT perfusion using outcome measures of delayed cerebral ischemia in aneurysmal subarachnoid hemorrhage, AJNR Am. J. Neuroradiol 34 (2) (Feb. 2013) 292–298, https://doi.org/10.3174/ajnr.A3225.
[54] W. Chai, X. Sun, F. Lv, B. Wan, L. Jiang, Clinical study of changes of cerebral microcirculation in cerebral vasospasm after SAH, in: Early Brain Injury or Cerebral Vasospasm, Springer, Vienna, 2011, pp. 225–228, https://doi.org/10.1007/978-3-7091-0353-1_39. Vienna.
[55] S. Payabvash, et al., Regional ischemic vulnerability of the brain to hypoperfusion: the need for location specific computed tomography perfusion thresholds in acute stroke patients, Stroke 42 (5) (May 2011) 1255–1260, https://doi.org/10.1161/STROKEAHA.110.600940.
[56] M.W. Cole, S. Pathak, W. Schneider, Identifying the brain's most globally connected regions, Neuroimage 49 (4) (Feb. 2010) 3132–3148, https://doi.org/10.1016/J.NEUROIMAGE.2009.11.001.
[57] D.J. Sharp, G. Scott, R. Leech, Network dysfunction after traumatic brain injury, Nature Reviews Neurol. 10 (3) (Feb. 2014) 156–166, https://doi.org/10.1038/nrneurol.2014.15, 10:3.
[58] R. Leech, D.J. Sharp, The role of the posterior cingulate cortex in cognition and disease, Brain 137 (1) (2014) 12, https://doi.org/10.1093/BRAIN/AWT162.
[59] F.A. Sehba, R.M. Pluta, Aneurysmal subarachnoid hemorrhage models: do they need a fix? Stroke Res. Treat. 2013 (Jun. 2013) 615154 https://doi.org/10.1155/2013/615154.
[60] S. Shiav, "Nitrite: A Physiological Store of Nitric Oxide and Modulator of Mitochondrial Function,", 2013, https://doi.org/10.1016/j.redox.2012.11.005.
[61] E. Franko, M. Ezra, D.C. Crockett, O. Joly, K. Pattinson, Effect of nitrite on the electroencephalographic activity in the healthy brain, Nitric Oxide 90 (Sep. 2019) 47–54, https://doi.org/10.1016/j.niox.2019.06.002.
[62] F.A. Sehba, V. Friedrich, Early micro vascular changes after subarachnoid hemorrhage, in: Early Brain Injury or Cerebral Vasospasm, vol. 110, Springer, Vienna, 2011, pp. 49–55, https://doi.org/10.1007/978-3-7091-0353-1_9. Pt 1, Vienna.
[63] G.W. Britz, et al., Time-dependent alterations in functional and pharmacological arteriolar reactivity after subarachnoid hemorrhage, Stroke 38 (4) (Apr. 2007) 1329–1335, https://doi.org/10.1161/01.STR.0000259853.43084.03.
[64] B. Friedrich, F. Müller, S. Feiler, K. Schöller, N. Plesnila, Experimental subarachnoid hemorrhage causes early and long-lasting microarterial constriction and microthrombosis: an in-vivo microscopy study, J. Cerebr. Blood Flow Metabol. 32 (3) (Mar. 2012) 447–455, https://doi.org/10.1038/jcbfm.2011.154.
[65] J.J. Heit, et al., Reduced intravoxel incoherent motion microvascular perfusion predicts delayed cerebral ischemia and vasospasm after aneurysm rupture, Stroke 49 (3) (Mar. 2018) 741–745, https://doi.org/10.1161/STROKEAHA.117.020395.
[66] C. de Wit, B. Jahrbeck, C. Schäfer, S.S. Bolz, U. Pohl, Nitric oxide opposes myogenic pressure responses predominantly in large arterioles in vivo, Hypertension 31 (3) (Mar. 1998) 787–794, https://doi.org/10.1161/01.hyp.31.3.787.
[67] M. Szekeres, G. Kaley, G. Nádasy, L. Dézsi, Nitric oxide modulates the interaction of pressure-induced wall mechanics and myogenic response of rat intramural coronary arterioles, Acta Physiol. Hung. 93 (1) (Mar. 2006) 1–12, https://doi.org/10.1556/APhysiol.93.2006.1.1.
[68] M. Sabri, J. Ai, K. Lakovic, J. D'abbondanza, D. Ilodigwe, R.L. Macdonald, Mechanisms of microthrombi formation after experimental subarachnoid hemorrhage, Neuroscience 224 (Nov. 2012) 26–37, https://doi.org/10.1016/j.neuroscience.2012.08.002.
[69] K.L. Davenpeck, T.W. Gauthier, A.M. Lefer, Inhibition of endothelial-derived nitric oxide promotes P-selectin expression and actions in the rat microcirculation, Gastroenterology 107 (4) (Oct. 1994) 1050–1058, https://doi.org/10.1016/0016-5085(94)90229-1.

[70] Q. Li, et al., Hemoglobin induced NO/cGMP suppression deteriorate microcirculation via pericyte phenotype transformation after subarachnoid hemorrhage in rats, Sci. Rep. 6 (1) (Feb. 2016) 22070, https://doi.org/10.1038/srep22070.
[71] N.A. Terpolilli, et al., Nitric oxide inhalation reduces brain damage, prevents mortality, and improves neurological outcome after subarachnoid hemorrhage by resolving early pial microvasospasms, J. Cerebr. Blood Flow Metabol. 36 (12) (Dec. 2016) 2096, https://doi.org/10.1177/0271678X15605848.
[72] J.O. Lundberg, E. Weitzberg, NO generation from inorganic nitrate and nitrite: role in physiology, nutrition and therapeutics, Arch Pharm. Res. (Seoul) 32 (8) (Aug. 2009) 1119–1126, https://doi.org/10.1007/S12272-009-1803-Z.
[73] D.A. Vitturi, R.P. Patel, Current perspectives and challenges in understanding the role of nitrite as an integral player in nitric oxide biology and therapy, Free Radic. Biol. Med. 51 (4) (Aug. 2011) 805–812, https://doi.org/10.1016/J.FREERADBIOMED.2011.05.037.
[74] N.A. Terpolilli, S.W. Kim, S.C. Thal, W.M. Kuebler, N. Plesnila, Inhaled nitric oxide reduces secondary brain damage after traumatic brain injury in mice, J. Cerebr. Blood Flow Metabol. 33 (2) (Feb. 2013) 311, https://doi.org/10.1038/JCBFM.2012.176.
[75] N.A. Terpolilli, et al., Inhalation of nitric oxide prevents ischemic brain damage in experimental stroke by selective dilatation of collateral arterioles, Circ. Res. 110 (5) (Mar. 2012) 727–738, https://doi.org/10.1161/CIRCRESAHA.111.253419.
[76] C. Fung, et al., Inhaled nitric oxide treatment for aneurysmal SAH patients with delayed cerebral ischemia, Front. Neurol. 13 (Feb) (2022), https://doi.org/10.3389/FNEUR.2022.817072.
[77] R.M. Pluta, A. Dejam, G. Grimes, M.T. Gladwin, E.H. Oldfield, Nitrite infusions to prevent delayed cerebral vasospasm in a primate model of subarachnoid hemorrhage, JAMA 293 (12) (Mar. 2005) 1477–1484, https://doi.org/10.1001/jama.293.12.1477.
[78] A.R. Fathi, R.M. Pluta, K.D. Bakhtian, M. Qi, R.R. Lonser, Reversal of cerebral vasospasm via intravenous sodium nitrite after subarachnoid hemorrhage in primates, J. Neurosurg. 115 (6) (Dec. 2011) 1213–1220, https://doi.org/10.3171/2011.7.JNS11390.
[79] J.R. Feiner, P.E. Bickler, Improved accuracy of methemoglobin detection by pulse CO-oximetry during hypoxia, Anesth. Analg. 111 (5) (Nov. 2010) 1160–1167, https://doi.org/10.1213/ANE.0b013e3181f46da8.